Supporting Information

Cologgi et al. 10.1073/pnas.1108616108

SI Materials and Methods

Culture Conditions. Cells were routinely revived from frozen stocks in NB medium (1) supplemented with 15 mM acetate and 40 mM fumarate (NBAF) and incubated at 30 °C. The cultures were transferred three times in fresh water (FW) medium (2), prepared with the modifications described below, and supplemented with 15 mM acetate and 40 mM fumarate (FWAF). The electron donor and acceptor were prepared as autoclaved concentrated stocks (0.75 M sodium acetate and 1 M sodium fumarate at pH 7, respectively). FW medium was prepared from a concentrated (10×) basal FW medium stock containing $NaHCO_3$ (25 g/L), $NaH_2PO_4 \cdot H_2O$ (0.6 g/L), NH_4Cl (2.5 g/L), and KCl (1.0 g/L). Vitamins were prepared as separate solutions as previously described (3). Trace minerals were prepared as previously described (4), except that $ZnSO_4$ was replaced with $ZnCl_2$ (0.13 g/L), and $Na_2WO_4 \cdot 2H_2O$ (0.025 g/L) was added. FWAF medium contained FW stock (96 mL/L), 0.75 M sodium acetate (20 mL/L), 1 M sodium fumarate (40 mL/L), vitamin solution (10 mL/L), and mineral solution (10 mL/L). The medium was dispensed in pressure tubes or serum bottles, sparged with N_2:CO_2 (80:20) to remove dissolved oxygen, and sealed with butyl rubber stoppers and aluminum tear-off seals (Wheaton) before autoclaving. Unless otherwise indicated, all cultures were incubated at 30 °C.

Pili Induction at Suboptimal Growth Temperatures. WT controls expressing pili (WT_{P+}) were obtained by growing WT cells at suboptimal growth temperatures (25 °C). Bacterial pili expression is often thermoregulated (5), an adaptive mechanism that enables bacteria to rapidly assemble the pili in environments where pili functions are advantageous (6). As in other bacteria (7), pili production in *Geobacter* is induced at suboptimal growth temperatures (25 °C) mimicking the suboptimal growth conditions that the cells encountered during the reduction of Fe(III) oxides (8). In contrast, growth at 30 °C prevents pili assembly and produces a pili-deficient strain, WT_{P-}.

EXAFS Analyses. The uranium EXAFS spectra were processed using the methods (9) in Athena (10) and modeled using FEFFIT (11) with theoretically generated models from FEFF 7.02 (12), as described elsewhere (13). Multiple scattering paths from distant C3 and Odist atoms were also included in the model, yet did not have a significant contribution. The coordination number for U-Oax (Noax values) obtained from EXAFS measurements of 3–4 biological replicates from at least two independent experiments was also used to estimate the amount of U(VI) reduced to U(IV) in each sample. For example, a Noax value of 0.3 was obtained for one of the biological replicates of the WT_{P+} (as given in Table S2), and 100% of U(VI) would have a U-Oax coordination number of 2.0. Therefore, the amount of U(VI) that corresponds to the WT_{P+} Noax is 0.3/2.0 = 0.15, which indicates that there is 15% U(VI) and 85% U(IV) in this sample.

Pili Purification, Quantification, and Biochemical Characterization. Pili were purified as detergent-insoluble fractions from cells first lysed by sonication and treated with RNase, DNase, and lysozyme enzymes (14). Three biological replicates were used for each strain. Cell membranes and proteins in the extracts were solubilized with SDS (1% final concentration) and separated by preparative 12% PAGE (5% stacking gel, 40 mA for 5 h) using a Prep Cell 491 apparatus (Bio-Rad). The detergent-insoluble fraction, which did not enter the stacking gel, was recovered by aspiration, washed in ddH_2O, extracted once with 95% ethanol (Decon Laboratories), and dried in a SpeedVac system (Savant Instruments Inc.) at room temperature for 20 min. The dry sample was resuspended in 1 mL of ddH_2O and vortexed for 60 s to break up large clumps before extracting and poorly bound, soluble protein with 0.2 M glycine (pH 1.5, adjusted with HCl; Invitrogen) at 100 °C for 10 min. The insoluble fraction was recovered by centrifugation (16, 000 × *g*, 25 min, 4 °C), washed five times with ddH_2O, and dried in a SpeedVac at room temperature before storing it at −20 °C. The amount of pili protein was measured after resuspending the dry samples in 10 mM *N*-cyclohexyl-2-aminoethanesulfonic acid buffer (pH 9.5), incubating at 4 °C overnight, and then mixing 1:1 with the working reagent solution of the Pierce Microplate BCA Protein Assay Kit (reducing agent compatible; Thermo Scientific). The samples were incubated at 60 °C for 1 h before spectrophotometric measurements. BSA was used as a standard.

For PAGE analyses, dried preparations of purified pili were resuspended in 5 μL of ddH_2O containing 10% (wt/vol) octyl-β-D-glucopyranoside (OG) (98%; Sigma) and incubated at room temperature for 2 h. The samples were diluted with 5 vol of ddH_2O to reduce the OG concentration to 2% (vol/vol) and incubated for an additional 24-h period at room temperature. The OG-treated sample was boiled in SDS/PAGE sample buffer (15) and subjected to electrophoresis through a 10–20% Tris/Tricine ReadyGel (Bio-Rad) using a Mini Protean Tetra Cell apparatus (Bio-Rad). After electrophoresis, the gels were silver stained using the Pierce Silver Stain for Mass Spectrometry kit (Thermo Scientific), following the instructions supplied by manufacturer, and scanned. The migration of the molecular mass standards in the gradient gel was estimated and fitted a polynomial distribution (R^2 = 0.95523), which was used to calculate the molecular mass of unknown bands. Duplicate gels were also electrophoretically transferred to a PVDF membrane (HyBond LFP; Amersham GE Healthcare) at 25 V for 150 min using a Mini Protean Tetra Cell apparatus (Bio-Rad). The Amersham ECL Plex Western blotting kit was used for the electrophoretic transfer and membrane blocking, following manufacturer's recommendations. After blocking, the membrane was incubated in 10 mL antibody diluent solution (90 min, room temperature, gentle agitation) containing a 1:5,000 dilution of the primary antibody (rabbit α-PilA polyclonal antibodies raised against the 42 C-t amino acids of *G. sulfurreducens* PilA protein) and a 1:2,500 dilution of goat α-rabbit IgG antibodies conjugated to the Cy^{tm} 5 fluorescence dye (ECL Plex; Amersham GE Healthcare). The membrane was washed 4 × 5 min in wash buffer [TBS-T (pH 7.40), 0.1% Tween 20] and rinsed three times in wash buffer without Tween 20. The protein bands that hybridized with the primary antibodies were visualized after scanning the membrane blot with a Typhoon imager operated in fluorescence mode (excitation at 633 nm, 670 BP 30 filter, and a photomultiplier setting at 600 V).

Gene Expression Analyses by qRT-PCR. Quantitative RT-PCR (qRT-PCR) was used to quantify *pilA* and *recA* transcripts in RNA extracted from resting cells of the WT_{P+} and WT_{P-} strains before and after incubation with uranyl acetate for 6 h. WT_{P+} controls incubated in the same reaction buffer without uranyl acetate were also included. RNA was extracted using the TRIzol reagent (Invitrogen) and treated with RQ1 RNase-free DNase (Promega) according to the manufacturer's instructions. Reverse transcription was performed using SuperScript III Reverse Transcriptase (Invitrogen) following manufacturer's recommendations. Primer

pairs RT_ORF02545_F and RT_ORF02545_R were used for *pilA* (16), and recA660f and recA737r were used for *recA* (17). For qRT-PCR, the cDNA generated after reverse transcription was diluted 1:1,000 in a 25-μL reaction that contained each primer (5 μM) and SYBR Green MasterMix (Applied Biosystems) according to the manufacturer's instructions. Samples were amplified using a Bio-Rad iCycler (iQ5 Multicolor Real-Time PCR Detection System). The comparative C_T method (18) was used to calculate the relative expression of the *pilA* gene using the *recA* constitutive expression as an internal control. Briefly, the ΔC_t value $[C_{T(pilA)} - C_{T(recA)}]$ was calculated for triplicate biological replicates before (0 h) and after (6 h) incubation with U(VI) acetate. The average of the difference between the 6 h and 0 h C_T values was used to calculate the $\Delta\Delta C_T$. The relative fold change in *pilA* expression vs. the *recA* internal control was calculated with the equation $2^{-}\Delta\Delta C_T$.

Transmission Electron Microscopy (TEM) and Confocal Laser Scanning Microscopy (CLSM) Analyses of Purified Pili. Detergent-insoluble fractions were examined by TEM and CLSM. For TEM, an aqueous solution of purified pili was adsorbed on a carbon-copper grid (Mesh 300; Electron Microscopy Sciences), negatively stained with 1% (wt/vol) uranyl acetate in distilled water, and examined with a JEOL 100 CX electron microscope (Japan Electron Optic Laboratory) operated at 100 kV. For CLSM, detergent-insoluble fractions were dissolved in PBS (pH 7), adsorbed onto glass coverslips for 30 min, washed with PBS, and fixed with 3.7% paraformaldehyde in PBS. The samples were then incubated for 30 min in PBS-1% BSA before overnight incubation at 4 °C with a 1:100 dilution anti-PilA primary antibody in PBS-1% BSA. After three washes in PBS-1% BSA, the samples were incubated with a 1:1,000 dilution of anti-rabbit antibodies conjugated to the Alexa fluor 488 dye (Invitrogen) for 1 h. The coverslips were then washed three times with PBS and examined with a Zeiss LSM Pascal confocal microscope equipped with a Plan-Neofluar 63× oil objective (excitation 488 nm; emission 505–535 nm).

TEM and Energy Dispersive Spectroscopy (EDS) Analyses. Cells from resting-cell suspensions incubated for 6 h with uranyl acetate were adsorbed onto 300-mesh carbon-coated copper grids (Ted Pella), fixed with 1% glutaraldehyde for 5 min, and washed three times with ddH_2O for 2 min. Imaging and elemental analysis of the extracellular uranium precipitates were performed with a JEOL 2200FS operated at 200 kV and an EDS detector.

For thin sections, cells were harvested by centrifugation (1,200 × *g*, 30 min, room temperature) and prepared as previously described (19), except that a Power Tome XL (RMC Products, Boeckeler Instruments) was used for sample sectioning. Thin sections were imaged with a JEOL 100CX operated at 80 kV. Approximately 400–500 cells from randomly taken, thin-sectioned fields were also examined for periplasmic mineralization. A cell was considered to have a mineralized periplasm when it contained both a fully mineralized outer membrane and generalized mineralization in the periplasm and/or inner membrane.

SDS/PAGE and Staining of Outer Membrane, Heme-Containing Proteins. Outer membrane *c*-cytochromes were mechanically detached from all of the strains and isolated as previously described (20). A mutant deficient in the outer membrane *c*-cytochrome OmcS (20) and grown at 25 °C was included as a control. Proteins (2.5 μg) in the supernatant fluids were separated by Tris-glycine denaturing PAGE (21) using a 12% Mini-Protean TGX gel (Bio-Rad). The Novex Sharp molecular weight markers (Invitrogen) were used as standards. Reducing agents were omitted from the SDS sample buffer, and the samples were loaded onto the gel without boiling to prevent the loss of heme groups (22). *C*-type cytochromes were detected as heme-stained bands using *N*,*N*,*N*′,*N*′-tetramethylbenzidine, as previously described (22). After heme staining, the gels were photographed, destained with 70 mM sodium sulphite (22), and silver stained for total protein with the Pierce Silver Stain Kit for MS (Thermo Scientific).

1. Coppi MV, Leang C, Sandler SJ, Lovley DR (2001) Development of a genetic system for *Geobacter sulfurreducens*. *Appl Environ Microbiol* 67:3180–3187.
2. Lovley DR, Phillips EJ (1988) Novel mode of microbial energy metabolism: Organic carbon oxidation coupled to dissimilatory reduction of iron or manganese. *Appl Environ Microbiol* 54:1472–1480.
3. Balch WE, Fox GE, Magrum LJ, Woese CR, Wolfe RS (1979) Methanogens: Reevaluation of a unique biological group. *Microbiol Rev* 43:260–296.
4. Lovley DR, Greening RC, Ferry JG (1984) Rapidly growing rumen methanogenic organism that synthesizes coenzyme M and has a high affinity for formate. *Appl Environ Microbiol* 48:81–87.
5. Göransson M, Forsman K, Uhlin BE (1989) Regulatory genes in the thermoregulation of *Escherichia coli* pili gene transcription. *Genes Dev* 3:123–130.
6. Silverman M, Belas R, Simon M (1984) Genetic control of bacterial adhesion. *Microbial Adhesion and Aggregation*, ed Marshall KC (Springer, Berlin), pp 95–107.
7. Sahu SN, et al. (2003) The bacterial adaptive response gene, *barA*, encodes a novel conserved histidine kinase regulatory switch for adaptation and modulation of metabolism in *Escherichia coli*. *Mol Cell Biochem* 253:167–177.
8. Reguera G, et al. (2005) Extracellular electron transfer via microbial nanowires. *Nature* 435:1098–1101.
9. Newville M (2001) IFEFFIT: Interactive EXAFS analysis and FEFF fitting. *J Synch Rad* 8: 322–324.
10. Ravel B, Newville M (2005) ATHENA, ARTEMIS, HEPHAESTUS: Data analysis for X-ray absorption. *J Synch Rad* 12:537–541.
11. Stern EA, Heald SM (1983) Basic principles and applications of EXAFS. *Handbook of Synchrotron Radiation*, ed Koch EE (North-Holland, New York), Vol 10, pp 995–1014.
12. Zabinsky SI, Rehr JJ, Ankudinov A, Albers RC, Eller MJ (1995) Multiple-scattering calculations of X-ray-absorption spectra. *Phys Rev B* 52:2995–3009.
13. Kelly SD, et al. (2008) Speciation of uranium in sediments before and after in situ biostimulation. *Environ Sci Technol* 42:1558–1564.
14. Collinson SK, Emödy L, Müller KH, Trust TJ, Kay WW (1991) Purification and characterization of thin, aggregative fimbriae from *Salmonella enteritidis*. *J Bacteriol* 173:4773–4781.
15. Schägger H, von Jagow G (1987) Tricine-sodium dodecyl sulfate-polyacrylamide gel electrophoresis for the separation of proteins in the range from 1 to 100 kDa. *Anal Biochem* 166:368–379.
16. Nevin KP, et al. (2009) Anode biofilm transcriptomics reveals outer surface components essential for high density current production in *Geobacter sulfurreducens* fuel cells. *PLoS ONE* 4:e5628.
17. Holmes DE, et al. (2006) Microarray and genetic analysis of electron transfer to electrodes in *Geobacter sulfurreducens*. *Environ Microbiol* 8:1805–1815.
18. Schmittgen TD, Livak KJ (2008) Analyzing real-time PCR data by the comparative $C_{(T)}$ method. *Nat Protoc* 3:1101–1108.
19. Marshall MJ, et al. (2006) *c*-Type cytochrome-dependent formation of U(IV) nanoparticles by *Shewanella oneidensis*. *PLoS Biol* 4:e268.
20. Mehta T, Coppi MV, Childers SE, Lovley DR (2005) Outer membrane *c*-type cytochromes required for Fe(III) and Mn(IV) oxide reduction in *Geobacter sulfurreducens*. *Appl Environ Microbiol* 71:8634–8641.
21. Ausubel FM, et al., eds (1995) *Current Protocols in Molecular Biology* (Wiley, New York), Vol 2.
22. Thomas PE, Ryan D, Levin W (1976) An improved staining procedure for the detection of the peroxidase activity of cytochrome P-450 on sodium dodecyl sulfate polyacrylamide gels. *Anal Biochem* 75:168–176.

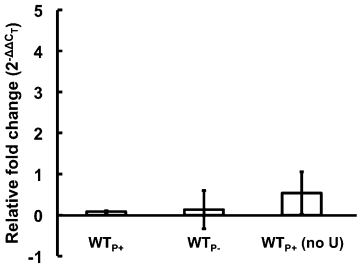

Fig. S1. Fold change expression of *pilA* relative to *recA* in resting-cell suspensions of the WT_{P+} and WT_{P-} strains after 6 h of incubation with 1 mM U(VI) acetate. A WT_{P+} control incubated in reaction buffer without U(VI) acetate is also shown [WT_{P+} (no U)].

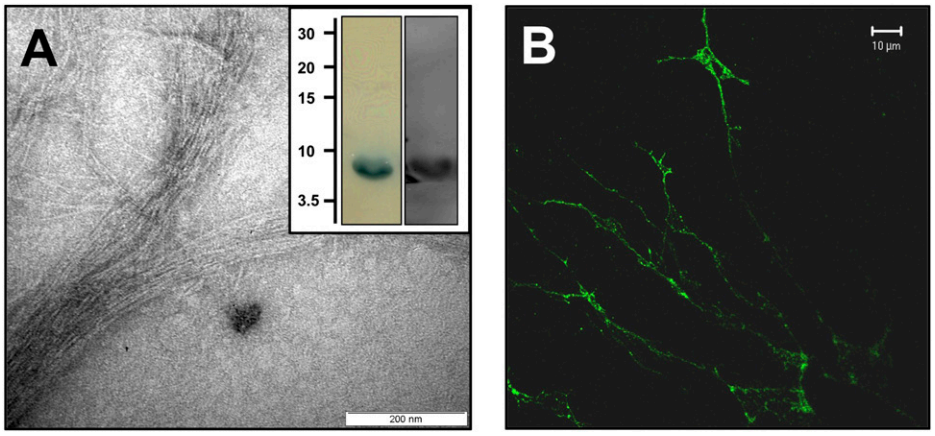

Fig. S2. TEM (*A*) and CLSM (*B*) micrographs of, respectively, negatively stained and anti-PilA immunodetected pilus fibers isolated as detergent-insoluble fractions in the WT_{P+}. (*A Inset*) SDS/PAGE Tricine gel (*Left*) and Western blot using anti-PilA polyclonal antibodies (*Right*) showing the depolymerization of the purified pili into the PilA peptide subunits. Numbers at *Left* are molecular mass standards in KDa and were used to estimate the apparent mass of the PilA band (6.6 kDa, as predicted for the mature PilA based on amino acid sequence).

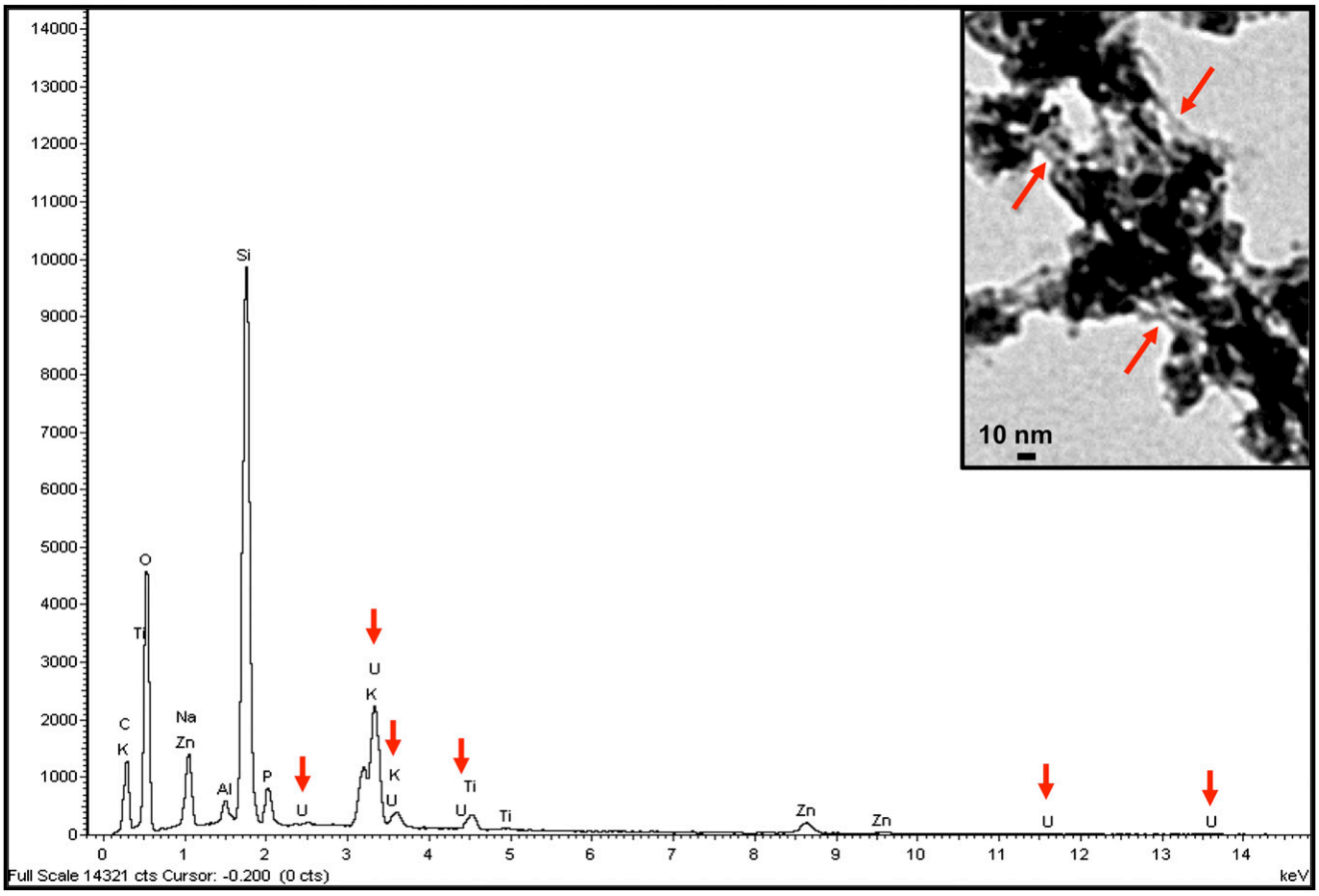

Fig. S3. Energy dispersive X-ray spectrum of the pili-associated electron-dense deposits imaged by TEM (*Inset*). Uranium peaks are highlighted with arrows. *Inset* shows pili filaments (red arrows) interspersed with the electron-dense uranium deposits.

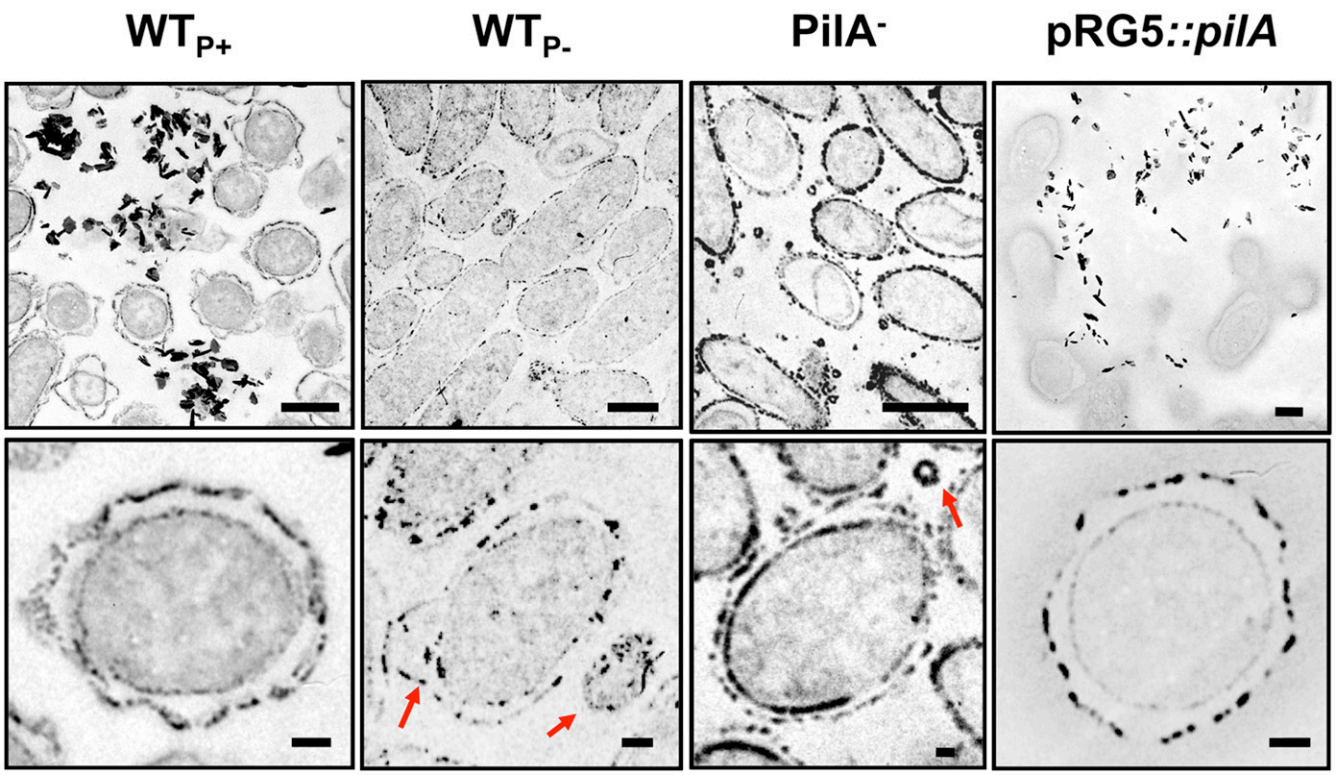

Fig. S4. Subcellular localization of uranium deposits by TEM analyses of thin sections of piliated (WT_{P+} and pRG5::*pilA*) and nonpiliated (WT_{P-} and $PilA^-$) cells. (*Upper*) Large fields. (Scale bar, 500 nm.) (*Lower*) Close-ups of a representative cell. (Scale bar, 100 nm.) Needle-like extracellular precipitates are noticeable in the *Upper* micrographs of the piliated strains, which is consistent with pili-associated uranium deposits. Discreet uranium deposits on the outer membrane are also noticeable in most cells of the WT_{P+} and WT_{P-}, and in a few cells of the pRG5::*pilA* strain, whereas fully mineralized outer membranes and periplasmic deposition is observed in most $PilA^-$ cells (*Upper* and *Lower*). Mineralized membrane vesicles budding from the cell (WT_{P-}) or detached ($PilA^-$) are indicated with red arrows.

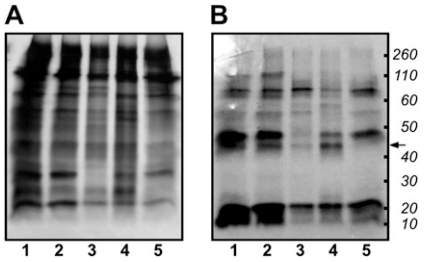

Fig. S5. SDS/PAGE profiling of mechanically detached outer membrane proteins. Samples were resolved in 12% (wt/vol) SDS/PAGE gels and silver stained for total protein (*A*) and heme content (*B*). Approximately 2.5 μg of protein were loaded per lane. Lane 1, WT_{P+}; 2, WT_{P-}; 3, $PilA^-$ mutant; 4, pRG5::*pilA*; and 5, $OmcS^-$ mutant. Numbers at *Right* are molecular weight standards in kilodaltons. The migration of the OmcS *c*-cytochrome is marked with an arrow.

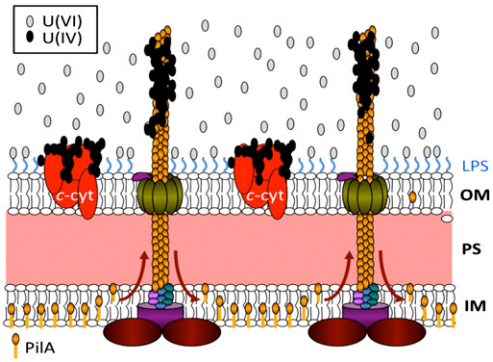

Fig. S6. Model for the extracellular reduction of U(VI) to U(IV) with conductive pili functioning as primary uranium reductases and *c*-cytochrome foci (*c*-cyt) as secondary reduction sites. IM, inner membrane; PS, periplasmic space; OM, outer membrane; LPS, lipopolysaccharide; PilA, pilin subunit.

Table S1. EXAFS modeling results for *R* and σ^2*

Path	CN	R, Å	σ^2 ($\cdot 10^{-3}$ Å^2)
Oax	Noax	1.79 ± 0.01	2†
Oeq	Noeq	2.37 ± 0.01	15 ± 1
C1	Nc1	2.94 ± 0.01	5 ± 2
C2	Nc2	3.43 ± 0.01	5 ± 2
Oax1-Oax2	Noax	3.58 ± 0.01	4†
Oax1-U-Oax2	Noax	3.58 ± 0.01	4†
Oax1-U-Oax1	2Noax	3.58 ± 0.01	8†
P1*	Np1	3.57 ± 0.05	5 ± 2
C3	Nc1	4.41 ± 0.02	5 ± 2
C1-C3	2Nc1	4.41 ± 0.02	5 ± 2
C1-C3-C1	Nc1	4.41 ± 0.02	5 ± 2
Odist	Nc2	4.55 ± 0.02	5 ± 2
C2-Odist	2Nc2	4.58 ± 0.02	5 ± 2
C2-Odist-C2	Nc2	4.60 ± 0.02	5 ± 2

CN, coordination number.
*PilA$^-$ mutant dataset only.
†Value held.

Table S2. EXAFS modeling results for coordination numbers

Dataset	Noax	Noeq	C1	P1	C2
WT_{P+}	0.3 ± 0.1	7.6 ± 0.4	1.8 ± 0.3	—	2.5 ± 0.4
WT_{P-}	0.4 ± 0.1	7.5 ± 0.3	1.7 ± 0.3	—	2.5 ± 0.4
PilA$^-$	0.9 ± 0.1	7.1 ± 0.4	2.0 ± 0.4	0.5 ± 0.3	2.3 ± 0.5
pRG5::*pilA*	0.8 ± 0.1	7.1 ± 0.4	1.6 ± 0.3	—	2.3 ± 0.5